Supplemental Information

Inventory of Supplemental Information

Supplemental Data

Table S1, related to Figure 1**.** ITC Measurement for the Titration of cIAP2 to TRAF2 at 25°C

TRAF2 (mM)	cIAP2 (mM)	K_A ($10^5 M^{-1}$)	K_D (μM)	ΔG (kcal/mol)	ΔH (kcal/mol)	$-T\Delta S$ (kcal/mol)	N
0.10	0.74	6.0±0.9	1.7	-7.88	-6.13±0.16	-1.75	0.30±0.006

Figure S1, related to Figure 1. Mapping of TRAF2 and cIAP2 interaction by co-expression. Non-tagged cIAP2 BIR1 domain (26-99) was co-expressed with various His-tagged TRAF2 constructs. The proteins were co-purified using Ni-affinity resin and assessed (if possible) by gel filtration to determine stable complex formation. The TRAF2 construct with residues 266-329 was shown to be necessary and sufficient for cIAP2 interaction.
(A). Summary.
(B). Pulldown.
(C). Gel filtration experiments.

A

TRAF2-His constructs	Expression level	Pulldown of cIAP2 BIR1
272-501	Low	Yes
272-346	Good	Yes
272-329	Good	Yes
272-317	Low	Yes
266-346	Good	Yes
266-329	Low	Yes
266-295	Very low	Yes

B

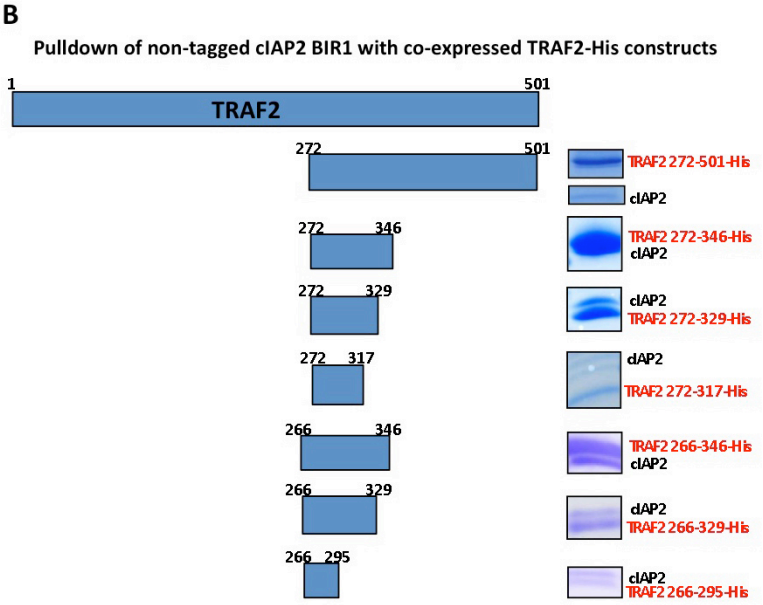

C

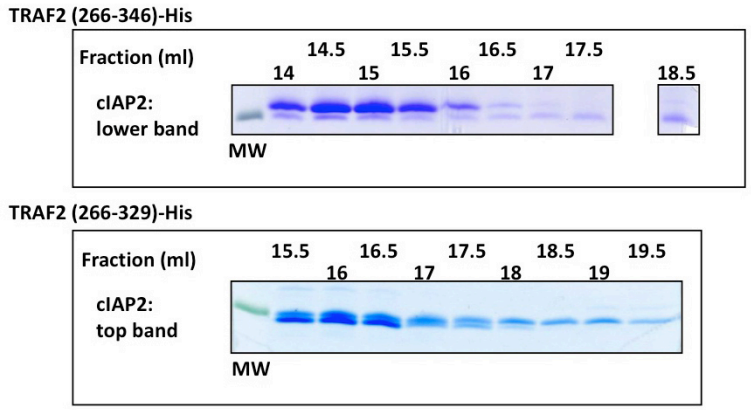

Figure S2, related to Table 1**.** Experimental Se-MAD map at 1.2 σ shown in stereo and in superposition with the final atomic model. Upper panel: a large region of the density map. Lower panel: a local region of the density map.

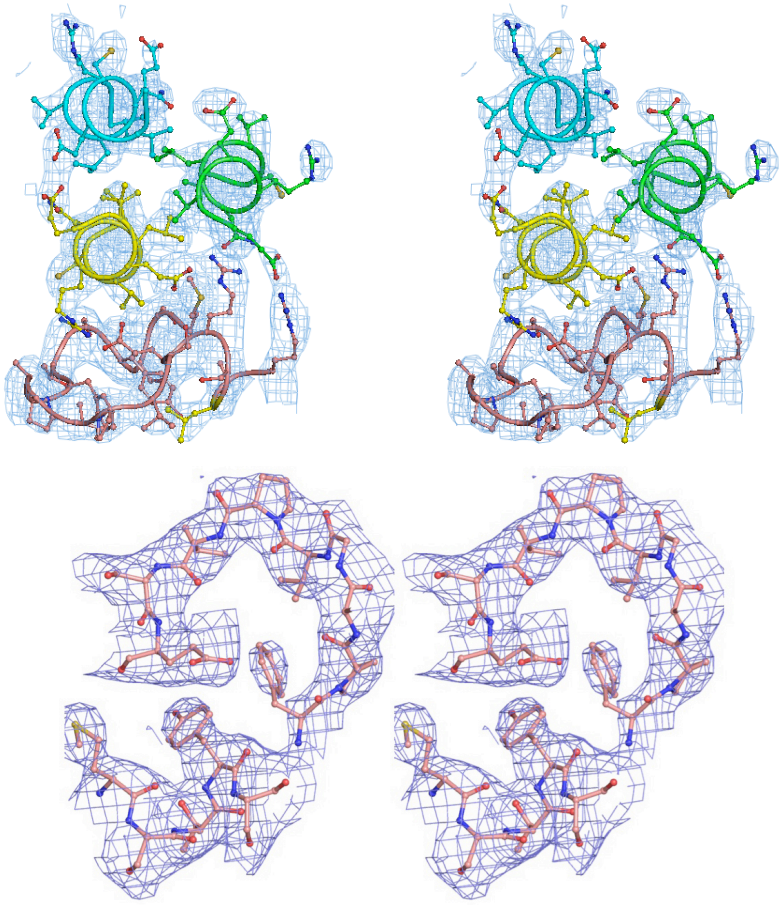

Table S2, related to Figure 4**.** Comparison of the original TRAF2: cIAP2 complex with the 3-fold rotated ones

	Original	Generated	Generated
Surface Area Burial	1,200 Å^2	930 Å^2	950 Å^2
# Interactions	113	81	98
Shape Complementarity Score	0.64	0.35	0.26

Table S3, related to Figure 4**.** ITC Measurement for the Titration of cIAP2 to TRAF1 at 25°C

TRAF1 (mM)	cIAP2 (mM)	K_A (10^3M^{-1})	K_D (μM)	ΔG (kcal/mol)	ΔH (kcal/mol)	-TΔS (kcal/mol)	N
0.12	1.08	9.0±4.1	111	-5.4	1.9±0.7	-7.2	0.96±0.21

Figure S3, related to Figure 4.
(A). Ribbon diagram and surface diagram of a hypothetical 3:3 TRAF2: cIAP2 complex, showing that the cIAP2 molecules do not overlap.
(B). ITC measurement for the interaction between TRAF1 and cIAP2.
(C). Measurement of the TRAF1: cIAP2 interaction using modified equilibrium dialysis.
(D). Formation of a TRAF1: $(TRAF2)_2$ heterotrimer even when TRAF1 is in excess.
(E). Two gel filtration fractions of somewhat different ratio mixtures of His-Smt3-TRAF1, His-TRAF2 and His-cIAP2 are shown. Most of the cIAP2 proteins co-migrated with the heterotrimer, less co-migrated with the TRAF2 trimer and almost nothing co-migrated with the TRAF1 trimer.

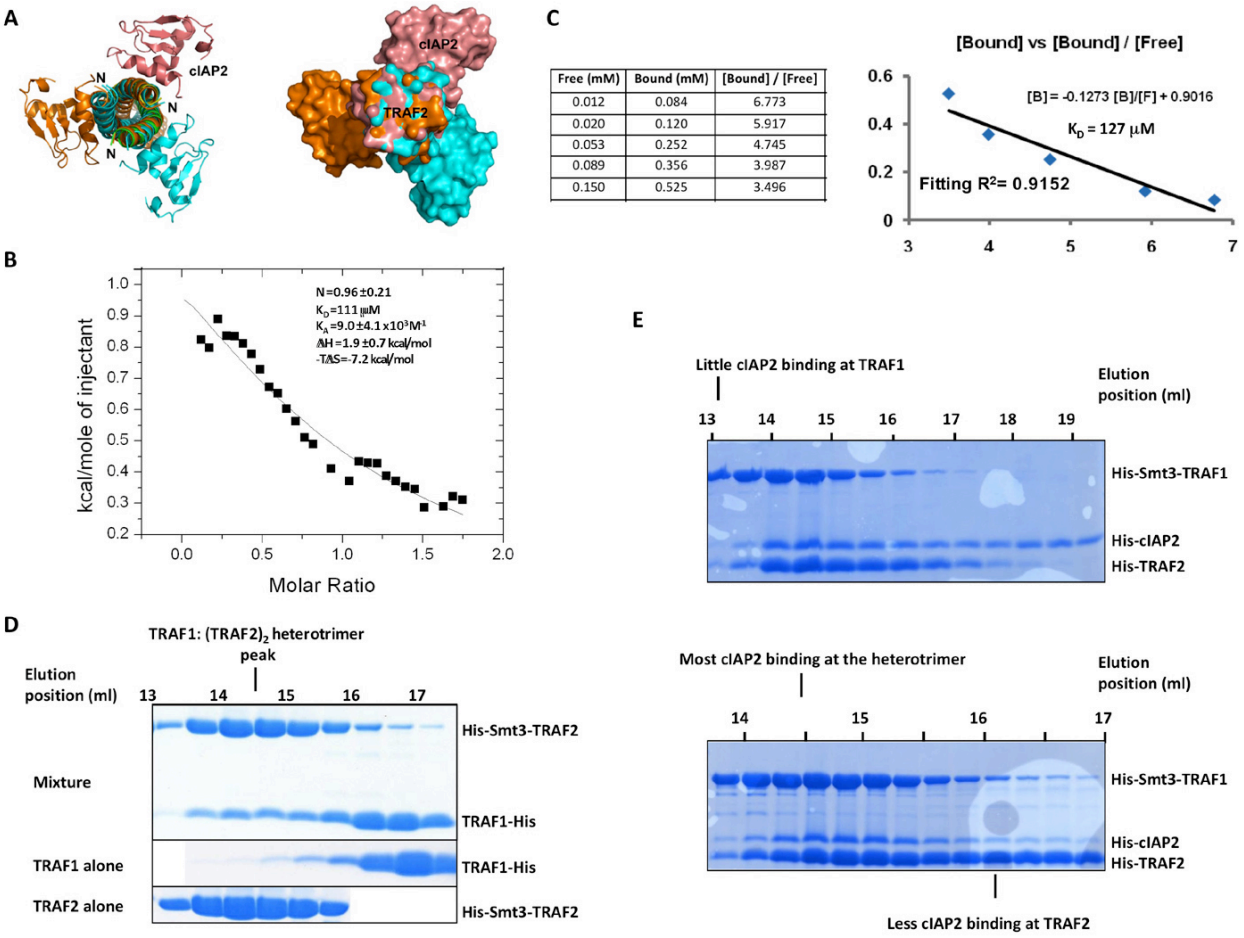

Figure. S4, related to Figure 5.
(A) A ribbon diagram of the TRAF1: TRAF2: cIAP2 ternary complex structure.
(B) Superposition of the TRAF trimer in the ternary complex structure with the TRAF trimer in the TRAF2: cIAP2 binary complex structure, showing the resulting orientational difference in the cIAP2 molecules. The TRAF2: cIAP2 complex is shown in magenta.

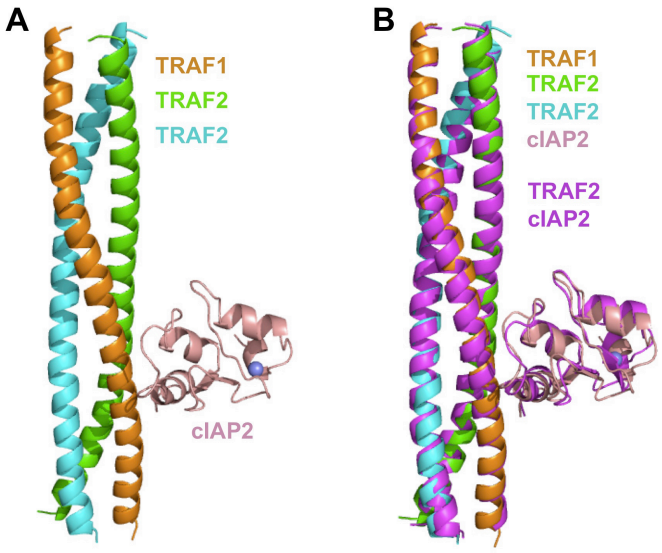

Table S4, related to Figure 5. Comparison of the original TRAF1: TRAF2: cIAP2 complex with the 3-fold rotated ones

	Original	Generated	Generated
Shape Complementarity Score	0.69	0.36	0.21

Supplemental Experimental Procedures

Protein Preparation. Human cIAP2 BIR1 domain (residues 26-99) and various human TRAF2 segments were cloned into pET26b in tandem to generate cIAP2: TRAF2-His co-expression constructs. There is a ribosomal binding site in front of each coding sequence. The cIAP2: TRAF2-His co-expression constructs were transformed into BL21 (DE3 RIPL) cells and cultured in LB medium at 37 ^{o}C. Protein expression was induced by IPTG (0.4 mM) when OD_{600} of the culture was 0.6. The cells were then grown at 20 ^{o}C for 16 hr. The proteins were purified with His-Pur^{TM} Cobalt Resin (PIERCE) followed by gel filtration with a Superdex 200 column (GE Biosciences). Similar cIAP2: TRAF1-His (residues 181-244) and cIAP2: TRAF1: TRAF2-His co-expression constructs were generated, expressed and purified using the protocol described for the cIAP2: TRAF2-His construct.

Human cIAP2 BIR1 domain (residues 26-99), TRAF1 (residues 181-244) and TRAF2 (residues 266-329) were cloned into pET28a or pET26b to produce N-terminally or C-terminally His-tagged proteins, His-cIAP2, TRAF1-His and His-TRAF2. Human TRAF2 (residues 266-329) and TRAF1 (residues 181-244) were cloned into pSUMO respectively to produce the fusion proteins, His-Smt3-TRAF2 and His-Smt3-TRAF1. There is a His tag and a Smt3 tag N-terminal to the TRAF2 and TRAF1 sequences. Untagged versions of cIAP2, TRAF1 and TRAF2 were also constructed. Expression and purification protocol for these constructs were as described for the cIAP2: TRAF2-His construct. All mutagenesis experiments were performed using the QuikChange® Site-Directed Mutagenesis Kit (Stratagene).

Crystallization and Structure Determination. The TRAF2: cIAP2 complex was initially crystallized by mixing 1 µl gel filtration purified protein (10 mg/ml in 20 mM Tris-HCl pH 8.0, 150 mM NaCl, and 5 mM DTT) with 1 µl of the reservoir solution containing 16 % PEG3350 and 8 % Tacsimate at pH 5.0 in a hanging drop vapor diffusion system at 20 ^{o}C. The initial crystals were used as seeds to produce better crystals in crystallization buffer containing 8 % PEG3350 and 6% Tacsimate at pH 5.0. Crystals were cross-linked with 50 % glutaldehyde for 10 minutes and briefly soaked into a cryo-solution containing 8 % PEG3350 and 6 % Tacsimate at pH 5.0 and 20 % glycerol before saved in liquid nitrogen. Crystals of both the complex and TRAF2 alone grew from the same samples and similar conditions. The TRAF1: $(TRAF2)_2$: cIAP2 complex was crystallized by mixing 1 µl gel filtration purified protein (10 mg/ml in 20 mM Tris-HCl pH 8.0, 150 mM NaCl, and 5 mM DTT) with 1 µl of the reservoir solution containing 0.15 M Ammonium sulfate, 0.1 M MES pH 6 and 15 % (w/v) PEG 4000 in a sitting drop vapor diffusion system at 4 °C.

All diffraction data were collected at the X25 and X29 beamlines of NSLS and processed with HKL2000 (Otwinowski and Minor, 1997) (Table 1). The structure of the TRAF2: cIAP2 complex was determined by multi-wavelength anomalous diffraction (MAD) (Hendrickson, 1985) of the intrinsic zinc atoms using the program SOLVE and RESOLVE (Terwilliger, 2004). The structures of TRAF2 alone and of the TRAF1: TRAF2: cIAP2 complex were solved by molecular replacement. Model building was performed in program Coot (Emsley and Cowtan, 2004). Refinement was done using CNS 1.2 (Brunger et al., 1998) and Refmac (Murshudov et al., 1997). Crystallographic statistics are shown in Table 1. All superpositions were performed with lsqman in the CCP4 suite (Collaborative Computational Project, 1994). Structural presentations were generated using Pymol (DeLano Scientific).

Multi-angle Light Scattering (MALS) Analyses. The protein samples were injected into a Superdex 200 (10/300 GL) gel filtration column (GE Healthcare) equilibrated in a buffer containing 20 mM Tris at pH 8.0 and 150 mM NaCl. The chromatography system was coupled to a three-angle light scattering detector (mini-DAWN TRISTAR) and a refractive index detector

(Optilab DSP) (Wyatt Technology). Data were collected every 0.5 s with a flow rate of 0.2 ml/min. Data analysis was carried out using ASTRA V.

Pulldown Assay. The cell pellets of WT and mutant His-Smt3 tagged TRAF2 (residues 266-329) were mixed with the cell pellet of non-tagged cIAP2 (residues 26-99). The mixtures were subjected to purification using the His-Pur^{TM} Cobalt Resin (PIERCE). The resin was washed extensively. The bound proteins were eluted and subjected to SDS-PAGE analysis. Similarly, the cell pellets of WT and mutant His-cIAP2 (residues 26-99) were mixed with the cell pellet of non-tagged Smt3-TRAF2 (residues 266-329) fusion protein. The mixtures were subjected to cobalt resin purification and the bound proteins were examined by SDS-PAGE. Non-tagged cIAP2 and non-tagged Smt3-TRAF2 did not bind the cobalt resin.

Isothermal Titration Calorimetry (ITC) and Data Analysis. Purified His-Smt3 tagged TRAF2 (residues 266-329), and His-tagged cIAP2 (residues 26-99) were subjected to gel filtration using a Superdex 200 HR10/30 column (GE Healthcare) in a buffer containing 20 mM Tris at pH 8.0 and 150 mM NaCl. ITC measurements were performed at 25 °C using iTC200 that was connected to a computer with ORIGIN software (Microcal Inc, Northampton, MA). Prior to titration, the protein samples were centrifuged at 13,000 rpm at 4 °C for 2 min to remove any debris. The calorimeter cell and titration syringe were extensively rinsed with buffer. For the TRAF2: cIAP2 interaction, the calorimetric titration was carried out at 25 °C with 16 injections of 2.4 µl 0.74 mM cIAP2, spaced 180 sec apart, into the sample cell containing a solution of 200 µl 0.10 mM TRAF2. A similar protocol was used for the ITC titration of cIAP2 (1.08 mM) into TRAF1 (0.12 mM) at 25°C, with 32 injections of 1.21 µl each and a spacing of 150 sec. The association constant (K_A), enthalpy change (ΔH) and the stoichiometry (N) were obtained by fitting the thermogram to a single binding site model using the ORIGIN software. The remaining thermodynamic parameters, the dissociation constant (K_D), the free energy change (ΔG), and the entropy change (ΔS) were calculated from the relationships:

$$K_A^{-1} = K_D \text{ and } -RT\ln K_A = \Delta G = \Delta H - T\Delta S$$

Modified Equilibrium Dialysis. His-cIAP2 was treated with thrombin to remove the His-tag and further purified by gel filtration in 150 mM NaCl and 20 mM Tris-HCl at pH 8.0. Modified equilibrium dialysis was performed similarly as previously described (Picollo et al., 2009). Purified His-smt-TRAF1 was incubated with Co^{2+} beads (pre-equilibrated in gel filtration buffer) for 1 h at 4^{o}C. The TRAF1 bound Co^{2+} beads were split to 50 µl aliquots, to which increasing concentrations of 50 µl non-tagged cIAP2 were added. After further incubation for 1 h at 4^{o}C with intermittently shaking, Co^{2+} beads were spun down. The concentration of free cIAP2 ([F]) was determined from the supernatant. The concentration of bound cIAP2 ([B]) was determined by subtracting that of free cIAP2 from that of total cIAP2. [B] was plotted as a function of [B] / [F] and fit to a straight line of [B] = constant – K_D [B] / [F].

Cell Biology Reagents. Antibodies against TRAF2, TRAF1 and IκBα were obtained from Santa Cruz Biotechnology. Antibodies against NIK and Myc were obtained from Cell Signaling Technology. All other reagents were from Sigma unless otherwise stated.

Cell Culture and Transfections. All reconstituted cell lines were generated as described previously (He et al., 2007). Briefly, HEK 293T cells were transfected with Moloney Murine Leukemia virus-ψA helper construct plus either pBABEpuro alone or the indicated pBABEpuro construct. *Traf2*$^{-/-}$, *Traf2Traf5*$^{-/-}$, or *NIK*$^{-/-}$ MEFs were then infected with the filtered 293T cell supernatants followed by selection with 2.5 µg/ml of puromycin. Transient transfection of HEK

293T cells was performed using the standard calcium phosphate method. For all transfection experiments CMV-β-gal was used as a normalization control.

Immunoprecipitation. Forty-eight hours after transfection, cells were lysed for 30 min at 4 °C in a modified radioimmune precipitation (mRIPA) buffer, containing 0.5 % (vol/vol) NP-40 and 0.1 % (wt/vol) sodium deoxycholate. Protease inhibitor cocktail (Sigma) was included in all lysates. The cell lysates were centrifuged for 10 min at 13,000 × g and the supernatant were incubated with anti-Flag M2 affinity gel (Sigma) for 2 hr. The immunoprecipitated complexes were separated by SDS-PAGE and blotted with the indicated antibodies.

Immunoblotting. Whole cells were lysed in 1 × SDS loading buffer (62.5 mM Tris-Cl, pH 6.8, 5 % β-mercaptoethanol, 2 % (wt/vol) SDS, 10 % (vol/vol) glycerol, and 0.1 % (wt/vol) bromophenol blue). SDS extracts were sonicated for 10 seconds using the Misonix Sonicator 3000 and then boiled for 5 minutes. Equal amounts of whole cell lysates were fractionated by 10 % SDS-PAGE, transferred to polyvinylidene fluoride membranes (Immobilon-P™) and immunoblotted with antibodies according to the manufacturer's recommended instructions. Primary antibodies were detected with either anti-rabbit or anti-mouse antisera conjugated to horseradish peroxidase (Santa Cruz) and visualized with electrochemiluminescence.

Supplemental References

Brunger, A.T., Adams, P.D., Clore, G.M., DeLano, W.L., Gros, P., Grosse-Kunstleve, R.W., Jiang, J.S., Kuszewski, J., Nilges, M., Pannu, N.S.*, et al.* (1998). Crystallography & NMR system: A new software suite for macromolecular structure determination. Acta Crystallogr *D54*, 905-921.

Collaborative Computational Project, N. (1994). The CCP4 Suite: Programs for Protein Crystallography. Acta Cryst *D50*, 760-763.

Emsley, P., and Cowtan, K. (2004). Coot: model-building tools for molecular graphics. Acta Crystallogr D Biol Crystallogr *60*, 2126-2132.

He, J.Q., Saha, S.K., Kang, J.R., Zarnegar, B., and Cheng, G. (2007). Specificity of TRAF3 in its negative regulation of the noncanonical NF-kappa B pathway. J Biol Chem *282*, 3688-3694.

Hendrickson, W.A. (1985). Analysis of protein structures from diffraction measurements at multiple wavelengths. Trans Am Crystallogr Assoc *21*, 11.

Murshudov, G.N., Vagin, A.A., and Dodson, E.J. (1997). Refinement of macromolecular structures by the maximum-likelihood method. Acta Crystallogr D Biol Crystallogr *53*, 240-255.

Otwinowski, Z., and Minor, W. (1997). Processing of X-ray diffraction data collected in oscillation mode. Methods Enzymol *276*, 307-326.

Picollo, A., Malvezzi, M., Houtman, J.C., and Accardi, A. (2009). Basis of substrate binding and conservation of selectivity in the CLC family of channels and transporters. Nat Struct Mol Biol *16*, 1294-1301.

Terwilliger, T. (2004). SOLVE and RESOLVE: automated structure solution, density modification and model building. J Synchrotron Radiat *11*, 49-52.